Palaeogeography, Palaeoclimatology, Palaeoecology 409 (2014) 33–47

Contents lists available at ScienceDirect

Palaeogeography, Palaeoclimatology, Palaeoecology

journal homepage: www.elsevier.com/locate/palaeo

Biome distribution over the last 22,000 yr in China

Jian Ni [a,b,c,*], Xianyong Cao [a,d], Florian Jeltsch [b,e,f], Ulrike Herzschuh [a,d]

[a] Alfred Wegener Institute Helmholtz Center for Polar and Marine Research, Research Unit Potsdam, Telegrafenberg A43, 14473 Potsdam, Germany
[b] Plant Ecology and Natural Conservation, Institute of Biochemistry and Biology, University of Potsdam, Maulbeerallee 2, 14469 Potsdam, Germany
[c] State Key Laboratory of Environmental Geochemistry, Institute of Geochemistry, Chinese Academy of Sciences, Guanshui Road 46, 550002 Guiyang, China
[d] Institute of Earth and Environmental Sciences, University of Potsdam, Karl-Liebknecht-Str. 24, 14476 Potsdam, Germany
[e] ZALF, Leibniz-Centre for Agricultural Landscape Research, Eberswalder Str. 84, 15374 Müncheberg, Germany
[f] Berlin-Brandenburg Institute of Advanced Biodiversity Research (BBIB), 14195 Berlin, Germany

A R T I C L E I N F O

Article history:
Received 12 September 2013
Received in revised form 19 April 2014
Accepted 30 April 2014
Available online 10 May 2014

Keywords:
Anthropogenic biome
Biomization
Holocene
Last glacial maximum
Plant functional types
Pollen dataset

A B S T R A C T

Patterns of past vegetation changes over time and space can help facilitate better understanding of the interactions among climate, ecosystem, and human impact. Biome changes in China over the last 22,000 yr (calibrated radiocarbon date, a BP) were numerically reconstructed by using a standard approach of pollen-plant functional type-biome assignment (biomization). The biomization procedure involves pollen data from 2434 surface sites and 228 fossil sites with a high quality of pollen count and ^{14}C dating, 51 natural and three anthropogenic plant functional types (PFTs), as well as 19 natural and one anthropogenic biome. Surface pollen-based reconstruction of modern natural biome patterns is in good agreement (74.4%) with actual vegetation distribution in China. However, modern large-scale anthropogenic biome reconstruction has not been successful based on the current setup of three anthropogenic PFTs (plantation, secondary, and disturbed PFT) because of the limitation of non-species level pollen identification and the difficulty in the clear assignment of disturbed PFTs. The non-anthropogenic biome distributions of 44 time slices at 500-year intervals show large-scale discrepant and changed vegetation patterns from the last glacial maximum (LGM) to the Holocene throughout China. From 22 ka BP to 19 ka BP, temperate grassland, xerophytic shrubland, and desert dominated northern China, whereas cold or cool forests flourished in central China. Warm–temperate evergreen forests were restricted to far southern China, and tropical forests were absent. During 18.5 ka BP to 12 ka BP, cold, cool, and dry biomes extended to some parts of northern, western, and eastern China. Warm–temperate evergreen and mixed forests gradually expanded to occupy the whole of southern China. A slight northward shift of forest biomes occurred from 15 ka BP to 12 ka BP. During 11.5 ka BP to 9 ka BP, temperate grassland and shrubland gradually stretched to northern and western China. Cold and cool forests widely expanded into northern and central China, as well as in the northern margin of South China along with temperate deciduous forest. Since the early mid-Holocene (approximately 8.5 ka BP to 5.5 ka BP), all forest biomes shifted northward at the expense of herbaceous and shrubby biomes. Simultaneously, cold and cool forest biomes occupied the marginal areas of the Tibetan Plateau and the high mountains in western China. During the middle to late Holocene, from 5 ka to the present, temperate grassland and xerophytic shrubland expanded to the south and east, whereas temperate deciduous forests slightly shifted southward. After 3 ka BP, forest biomes were absent in western China and on the Tibetan plateau surface. Dramatic biome shifts from the LGM to the Holocene were observed in the forest-grassland ecotone and transitional zones between temperate and subtropical climates, between subtropical and tropical regions, and in the mountainous margins of the eastern Tibetan Plateau. Evidence showed more human disturbances during the late Holocene. More pollen records and historical documents are therefore further needed to understand fully the human disturbance-induced large-scale forest changes. In addition, more classifications of anthropogenic biome or land cover, more distinct assignment of pollen taxa to anthropogenic PFTs, and more effective numerical and/or mechanistic techniques in building large-scale human disturbances are required.

1. Introduction

Global vegetation distribution has mainly been controlled by climate. However, both human-induced climate change and extensive human activities have altered the Earth's vegetation pattern in the Anthropocene (Alessa and Chapin, 2008; Ellis and Ramankutty, 2008; Ellis et al., 2010;

* Corresponding author at: Alfred Wegener Institute Helmholtz Center for Polar and Marine Research, Research Unit Potsdam, Telegrafenberg A43, 14473 Potsdam, Germany. Tel.: +49 331 288 2211.
E-mail address: jni@awi.de (J. Ni).

http://dx.doi.org/10.1016/j.palaeo.2014.04.023
0031-0182/

Ellis, 2011; Kaplan et al., 2011). Research on large-scale vegetation distribution in the past, present, and future, as well as the related driving forces, is therefore one of the research hot spots in the field of global change science. To understand comprehensively the effects of future climate scenarios and human disturbances on the Earth's vegetation and to assess the sensitivity and vulnerability of vegetation to climate change, insights into biome shifts from the past are necessary. Paleobiome reconstruction is essential to the understanding of past changes and interactions among vegetation, climate, and human disturbances, as well as for the evaluation of paleo-simulations of Earth system models.

The mapping of paleovegetation or paleobiome requires a reasonably high number of pollen records, which are mostly obtained from analyses of lake sediments, peat, and soils. With the use of biomization, a numerical method for transforming pollen taxa and percentages to biome types (Prentice et al., 1996), past biome geography from regional to continental and global scales has been synthesized (Prentice and Webb, 1998; Prentice et al., 2000). Paleobiome distributions have been commonly mapped for two time slices: the mid-Holocene (MH) and the LGM, representing the climate extremes in a warmer–wetter and colder–drier world, respectively (Prentice et al., 2000). However, biome mapping with suitably high temporal resolution to infer vegetation change in space and time remains lacking; in particular, a comprehensive view of biome distribution during the last deglaciation, both at the continental and global scales, is missing. Therefore, important questions concerning paleovegetation remain unaddressed: Have biome shifts in response to climate changes occurred in a similar manner, or do shifts differ in range and direction? Did regional similarity exist in biome transitional patterns among single climate change events? Did biome transitions occur synchronously with climate change, or can time lags be identified?

By contrast, past human impacts on vegetation were typically investigated only at local scales, such that the relevant question of whether human activities had already caused large-scale biome transition (e.g., Ellis and Ramankutty, 2008; Ellis et al., 2010; Ellis, 2011; Kaplan et al., 2011) before the Industrial Revolution remains debated (e.g., Dearing, 2006). Holocene land-cover change of the world has been reconstructed by the REVEALS model (Gaillard et al., 2010). In Europe, the anthropogenic land-cover change has been detected in Britain using a pollen-based pseudobiomization approach (Fyfe et al., 2010; Woodbridge et al., 2014). In Asia, a disturbed vegetation pattern has been reconstructed by applying the biomization method to Japanese pollen records (Gotanda et al., 2008). Pollen taxa-based synthesis showed that human land use, such as crop cultivation and deforestation, was a major driving factor of natural vegetation change in the late Holocene in northern East China (Ren, 2000). However, in these later two studies, anthropogenic biome transitions or shifts were not well determined.

With respect to millennial-scale paleobiome changes at a subcontinental scale and the related driving forces (Wang et al., 2010), China represents an ideal study region because of both its marked and extensively investigated climate change and its long and intensive human land use history. China's biome reconstructions have thus far been performed based on a small number of continuously updated pollen datasets, applying the biomization technique based on different schemes of PFTs (Yu et al., 1998, 2000; Chen et al., 2010; Ni et al., 2010). However, similar to the global studies focusing on the two time slices of the MH and LGM, no time-series numerical reconstructions of natural and anthropogenic biomes are available. In this work, a pollen-based quantitative reconstruction of paleobiome changes in China over the past 22,000 yr is presented by using the biomization method (Prentice et al., 1996) and a newly established pollen dataset (Cao et al., 2013).

2. Materials and methods

2.1. Pollen dataset

The modern pollen data were derived from a previous surface pollen dataset from China that includes 2324 pollen records (Chen et al., 2010) and 110 recently published pollen records of the Alashan Plateau of western Inner Mongolia (Herzschuh et al., 2004), the Qilian Mountains of the northeastern Tibetan Plateau (Herzschuh et al., 2006), and the Hengduan Mountains of the southeastern Tibetan Plateau (Kramer et al., 2010). In total, 2434 modern pollen records covering most regions of China were included in this present study (Fig. 1a).

The fossil pollen data were derived from the eastern continental Asia pollen dataset (see Table 1 in Cao et al., 2013 for more details), but in this study the 228 original records from China were used (raw or digitized data, with no removals and combinations of pollen samples, and linear interpolations of pollen percentages, deleting the marine core 17964 from the South China Sea; Fig. 1b). All pollen data have reasonably high resolutions and robust chronologies.

All surface and fossil pollen taxa were homogenized. Pollen percentages were re-calculated based on the total number of terrestrial pollen grains, excluding aquatic pollen and spores from ferns and algae, but including Cyperaceae (Cao et al., 2013).

2.2. Pollen-PFTs-biome assignment

We use the standard biomization procedure to assign pollen taxa to biomes (Prentice et al., 1996; Prentice and Webb, 1998) through a global classification system of PFTs (Harrison et al., 2010), as described in detail in Chen et al. (2010) and Ni et al. (2010), with some minor changes.

After removing the PFTs of aquatic plants and ferns that have no regional biome indication, 72 PFTs derived from the Chinese scheme of PFTs (Chen et al., 2010; Ni et al., 2010) remain. Among these PFTs, 51 indicative PFTs were finally used in defining biomes (Appendix 1). The assignment of some pollen taxa to PFTs was updated (Appendix 1) according to newly available floras and databases (for example, the Scientific Database of China Plant Species at http://www.plants.csdb.cn/eflora/default.aspx). Three PFTs related to human land use impact (defined as anthropogenic PFTs) were introduced in this paper (Appendix 2). These PFTs are plantation, secondary, and disturbed PFTs. The first two PFTs are proposed in a disturbed vegetation reconstruction in Japan (Gotanda et al., 2008). The plantation PFT is broadly defined in this work as large areas of cultivation, such as timbers and fruit trees, but excluding flowers, medicines, and street trees. The secondary PFT is defined as a group of trees and shrubs sprouting in deforested areas and/or abandoned fields. The disturbed PFT is defined as a group of plants that are associated with human settlements, i.e., crops, vegetables, and synanthropic plants. Three kinds of pollen taxa-anthropogenic PFTs assignments are set up. The theoretical setup assigns every possible pollen taxa to anthropogenic PFTs (the highest number of pollen taxa in a PFT). The practical setup assigns limited pollen taxa to anthropogenic PFTs (the lowest number of pollen taxa). An in-between setup (combining the theoretical and practical setups) is also applied (Appendix 2).

A total of 19 biomes and their definitions in terms of key PFTs in this study (Table 1) come from the biome used in previous biome reconstructions of China (Chen et al., 2010; Ni et al., 2010). The grass PFT is removed from the definition of tropical deciduous broad-leaved forest and woodland, temperate xerophytic shrubland, and three tundra biomes: prostrate dwarf-shrub tundra, erect dwarf-shrub tundra, and cushion forb tundra. If the grass PFT is included in the definition of these biomes, the biome of tropical deciduous broad-leaved forest and woodland, which shares some shrubby taxa (e.g., Euphorbiaceae and Fabaceae) with the temperate xerophytic shrubland, appears in some sites of northern temperate China. In many cases, temperate grassland in northern China is replaced by the temperate xerophytic shrubland. Similarly, the three tundra biomes, which share some shrubby and herbaceous PFTs with temperate grassland, are replaced in northern and northeastern China. The PFT of tree fern is removed from the definition of subtropical and tropical forests because this PFT includes only one pollen taxon and has very limited potential to determine these forests.

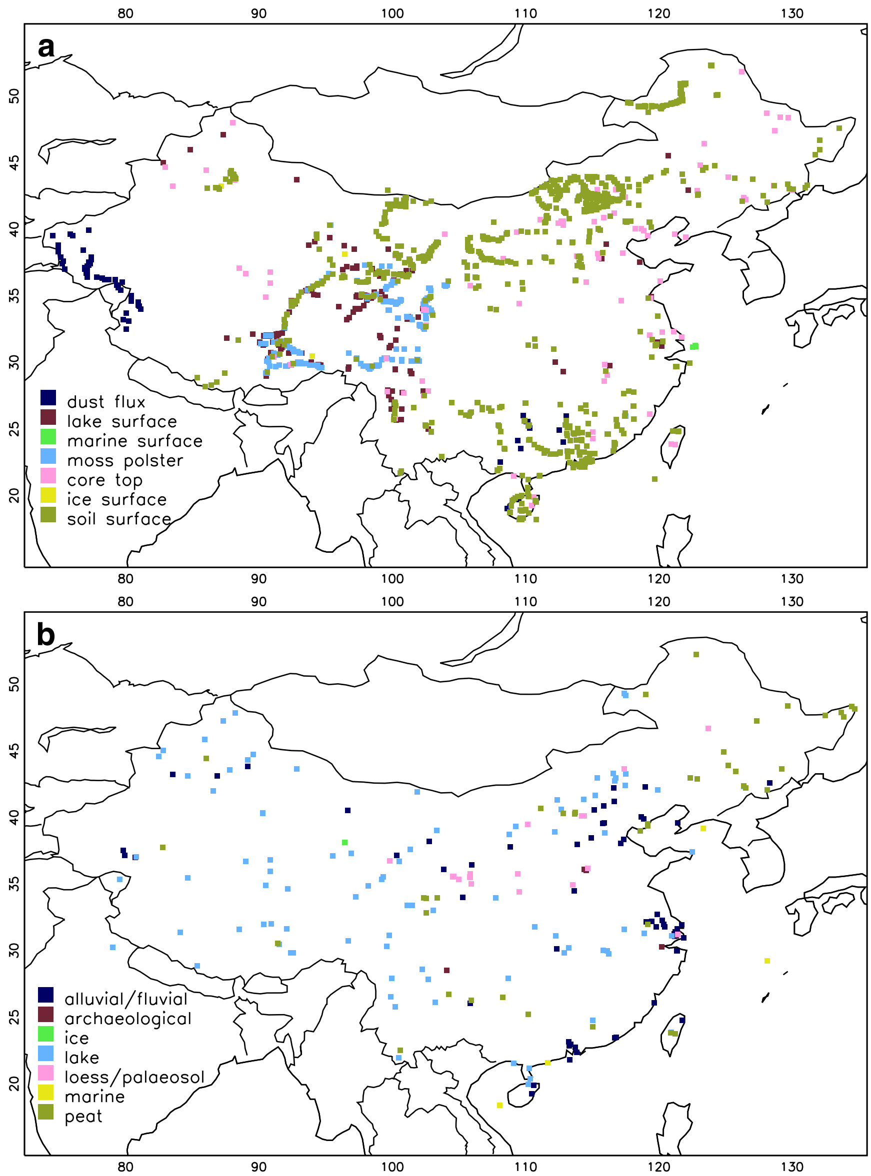

Fig. 1. Sampling site location and sediment type of modern surface pollen (a) and fossil pollen (b) in China.

In this work, an anthropogenic biome, defined by the plantation, secondary, and disturbed PFTs, is introduced (Table 1). However, unlike the Japanese disturbed vegetation reconstruction (Gotanda et al., 2008), not all herbaceous taxa are included to define a disturbed biome. Only reasonable herbaceous taxa are assigned to single anthropogenic PFTs (Appendix 2).

2.3. Mapping and analytical strategy

Biome maps from 500 calibrated years before present (cal a BP) to 22,000 cal a BP at 500-year intervals are plotted. Interpolated dating data on pollen samples cannot exactly match the target time slices. Therefore, a time span around the time slice (mapping time = time slice ± time span) should be set up. After testing the 50-, 100-, 150-, and 200-year time spans around each time slice, the time slice ± 150 yr is finally adopted as the mapping time to ensure sufficient sites for mapping. The average number of sampling sites for biome mapping is 130 ± 91 (13–306), of which 223 ± 45 (151–306) are before 10 ka BP, and 59 ± 36 (13–128) are after 10 ka BP. When one sampling site has several dating data within the same time span, the time nearest to the time slice (or sample with nearest time and frequently reconstructed biome) is selected.

3. Results

3.1. Modern biomes

The reconstructed modern biome pattern is in agreement with modern vegetation distribution in China at a level of 74.4% (Fig. 2a, b). Cold and cool temperate forests are mainly distributed in northeastern China and less scattered in the northern and western high mountains. Temperate deciduous forests are located at the middle part of eastern China, as well as in some mountainous areas in the north and west. Warm–temperate evergreen and mixed forests are distributed in southern China, including Taiwan and Hainan Islands. Tropical semi-evergreen forest and rainforest are distributed in the southernmost mainland and Hainan Island. Temperate grassland is predominantly found in northern and western China along the approximate 400 mm precipitation isoline. Temperate desert dominates the western part of northern China. Temperate xerophytic shrubland is distributed in central northern and northwestern China. Steppe tundra, dwarf tundra,

Table 1
Biomes and key PFTs that define each biome. The list of PFTs can be found in Appendices 1 and 2.

No	Biome code	Biome name	PFTs
1	CLDE	Cold deciduous forest	bo.cd.mb.t, bo.d.n.t, eu.e.n.t, bo.cd.mb.lhs, bo.e.mb.lhs
2	CLEG	Cold evergreen needle-leaved forest	bo.cd.mb.t, bo.d.n.t, bo.e.n.t, eu.e.n.t, bo.cd.mb.lhs, bo.e.mb.lhs
3	CLMX	Cold–temperate evergreen needle-leaved and mixed forest	bo.cd.mb.t, bo.d.n.t, c-te.e.n.t, eu.e.n.t, bo.cd.mb.lhs, bo.e.mb.lhs
4	COEG	Cool evergreen needle-leaved forest	bo.cd.mb.t, bo.d.n.t, c-te.e.n.t, eu.e.n.t, te-ft.cd.mb.t, bo.cd.mb.lhs, bo.e.mb.lhs
5	COMX	Cool mixed forest	bo.d.n.t, c-te.e.n.t, eu.e.n.t, te-ft.cd.mb.t, te-fa.cd.mb.t, bo.e.mb.lhs, te.cd.mb.lhs
6	TEDE	Temperate deciduous broad-leaved forest	bo.cd.mb.t, eu.e.n.t, te.e.n.t, te-fa.cd.mb.t, te-fi.cd.mb.t, te.cd.mb.lhs
7	WTEM	Warm–temperate evergreen broad-leaved and mixed forest	wt.e.mb.t, wt.e.n.t, wt.e.sb.t, wt.cd.mb.t, wt.d.n.t, te-fi.cd.mb.t, eu.e.n.t, wt.e.mb.lhs, wt.e.sb.lhs, wt.cd.mb.lhs
8	WTEG	Warm–temperate evergreen broad-leaved forest	wt.e.mb.t, wt.e.n.t, wt.e.sb.lhs, wt.e.sb.t, eu.e.n.t, wt.e.mb.lhs
9	TRSE	Tropical semi-evergreen broad-leaved forest	tr.e.mb.t, tr-m.dd.mb.t, wt.d.n.t, wt.e.mb.t, wt.e.n.t, wt.e.sb.t, tr.e.mb.lhs
10	TREG	Tropical evergreen broad-leaved forest	tr.e.mb.t, tr.e.sb.t, tu.t, wt.d.n.t, wt.e.mb.t, wt.e.n.t, wt.e.sb.t, tr.e.mb.lhs
11	TRDE	Tropical deciduous broad-leaved forest and woodland	tr-m.dd.mb.t, tr-x.dd.mb.t, tr-m.dd.mb.lhs, tr-x.dd.mb.lhs
12	TEXE	Temperate xerophytic shrubland	dt.sl.lhs, ml.t, sl.t, te-dt.fb
13	TEGR	Temperate grassland	di.sl.lhs, eu-dt.fb, g, s, te-dt.fb
14	DESE	Desert	cs, dt.sl.lhs, ft.ml.lhs, g, ha, lsuc, ssuc
15	CUSH	Cushion-forb tundra	ar.fb, rc.fb
16	DRYT	Graminoid and forb tundra	ar.fb, g, s
17	PROS	Prostrate dwarf-shrub tundra	ar.cd.mb.pds, ar.e.mb.pds, ar.fb
18	DWAR	Erect dwarf-shrub tundra	ar.cd.mb.eds, ar.cd.mb.pds, ar.e.mb.eds, ar.e.mb.pds, s
19	SHRU	Low and high shrub tundra	ar.cd.mb.eds, ar.cd.mb.lhs, ar.cd.mb.pds, ar.e.mb.eds, ar.e.mb.lhs, ar.e.mb.pds, ar.e.n.lhs, ar.e.n.pds, g, s
20	ANBI	Anthropogenic biome	pt, sd, dt

and shrub tundra are mainly located on the plateau surface and margin of Tibet (Fig. 2b). Despite the general fit of pollen-based biomes with those inferred from the vegetation atlas, some mismatch is evident. For example, the prostrate dwarf shrub tundra biome appears in some sites at the ecotone between cold or cool forests and temperate grassland and shrubland in northeastern China. Additionally, alpine tundra biomes on the Tibetan Plateau are sometimes confused with temperate grassland and desert (Fig. 2b). These problems mainly originate from the sharing of grass and shrub PFTs among these biomes.

The theoretical assignment of pollen taxa to anthropogenic PFTs (Appendix 2) produces anthropogenic biomes in 443 sites, which accounts for 18.2% of the total number of modern pollen sites. These anthropogenic sites are mostly located in forest-grassland areas of the eastern part of China (Fig. 2c). Such reconstruction reflects, to some extent, the greater human disturbance in eastern than western China, but the reconstruction is not reasonable because these anthropogenic sites are evenly distributed (Fig. 2c). The more restricted but practical assignment of pollen taxa to anthropogenic PFTs (Appendix 2) results in no anthropogenic biomes. The biome types and distributions under this condition are the same as the natural biomes (Fig. 2b). Using the in-between setup to assign pollen taxa to anthropogenic PFTs (Appendix 2), the anthropogenic biomes are only located at 10 sites, which are in central eastern and northeastern China (Fig. 2d). Numerous sites, which are obviously human disturbed, are not reconstructed as anthropogenic biomes (e.g., the archeological site of Dadiwan and various sites in the cities Nanjing and Shanghai in eastern China). This observation indicates that the current setup and assignment of pollen taxa to anthropogenic PFTs have less power to build up the anthropogenic biome in China.

3.2. Biome patterns over the past 22 ka BP

The distribution of biomes in China over the past 22,000 yr varied spatially and temporally (Fig. 3) and sometimes changed dramatically (Appendix 3).

3.2.1. LGM (22 ka to 19 ka)

Under the control of cold and dry climates, biomes in this period were dominated by temperate grassland in northern China, cold and cool forests in central China, and warm–temperate evergreen forest in far southern China. The flourishing temperate grassland (steppe), along with some temperate xerophytic shrubland and desert, occupied the northern part of China. Graminoid and forb tundra (steppe tundra), cushion-forb tundra, and dwarf shrub tundra rarely appeared in central China to the eastern and northern margin of the Tibetan Plateau in some time slices. Cold deciduous, cold evergreen needle-leaved, cool mixed, cool evergreen needle-leaved, and sometimes temperate deciduous forests exhibited a scattered distribution in central to northeastern China. Warm–temperate (subtropical) evergreen and mixed forests were located in only a few sites in far southern China. No tropical forests were present throughout the whole LGM (Fig. 3 and Appendix 3).

3.2.2. Last glacial (18.5 ka to 12 ka)

Compared with that in the LGM, vegetation in the last glacial period has the following features: Temperate grassland, xerophytic shrubland, and desert consistently dominated northern and western China, including the Tibetan Plateau. No tundra biomes were reconstructed before 13.5 ka BP, and fewer tundra biomes occurred between 13.5 ka BP and 12 ka BP on the Tibetan Plateau and the Inner Mongolian Plateau compared with that in the LGM. Cold and cool coniferous and mixed forests occupied central China, but more frequently appeared in northern, western, and eastern China, especially from 16 ka BP to 12 ka BP. Temperate deciduous forest sometimes occurred in eastern coastal areas of southern China, but warm–temperate (subtropical) evergreen and mixed forests gradually expanded from far southern China to the whole of southern China. Tropical semi-evergreen forest was reconstructed only once in southeastern China at 14 ka BP. An insufficient number of sampling sites hindered our ability to interpret biome boundary shifts on a finer spatial scale, but evidence still shows weak or strong biome shifts from 16 ka BP to 15 ka BP, particularly a slight trend of a northward shift of some forest biomes (Fig. 3 and Appendix 3).

3.2.3. Early Holocene (11.5 ka to 9 ka)

Temperate grassland, xerophytic shrubland, and desert still dominated a large area of northern and western China, including the Tibetan Plateau, but steppe and shrubland gradually shifted to the north and west. The tundra biome appeared in northern China and on the Tibetan Plateau. Cold and cool mixed forest and cool evergreen needle-leaved forest widely expanded into these areas, but also occurred in the central and northern parts of South China. In the northern margin of southern China, subtropical evergreen forest occurred but was mixed with temperate deciduous forest, particularly on the eastern coast. From 9.5 ka BP, tropical semi-evergreen and evergreen forests started to appear in

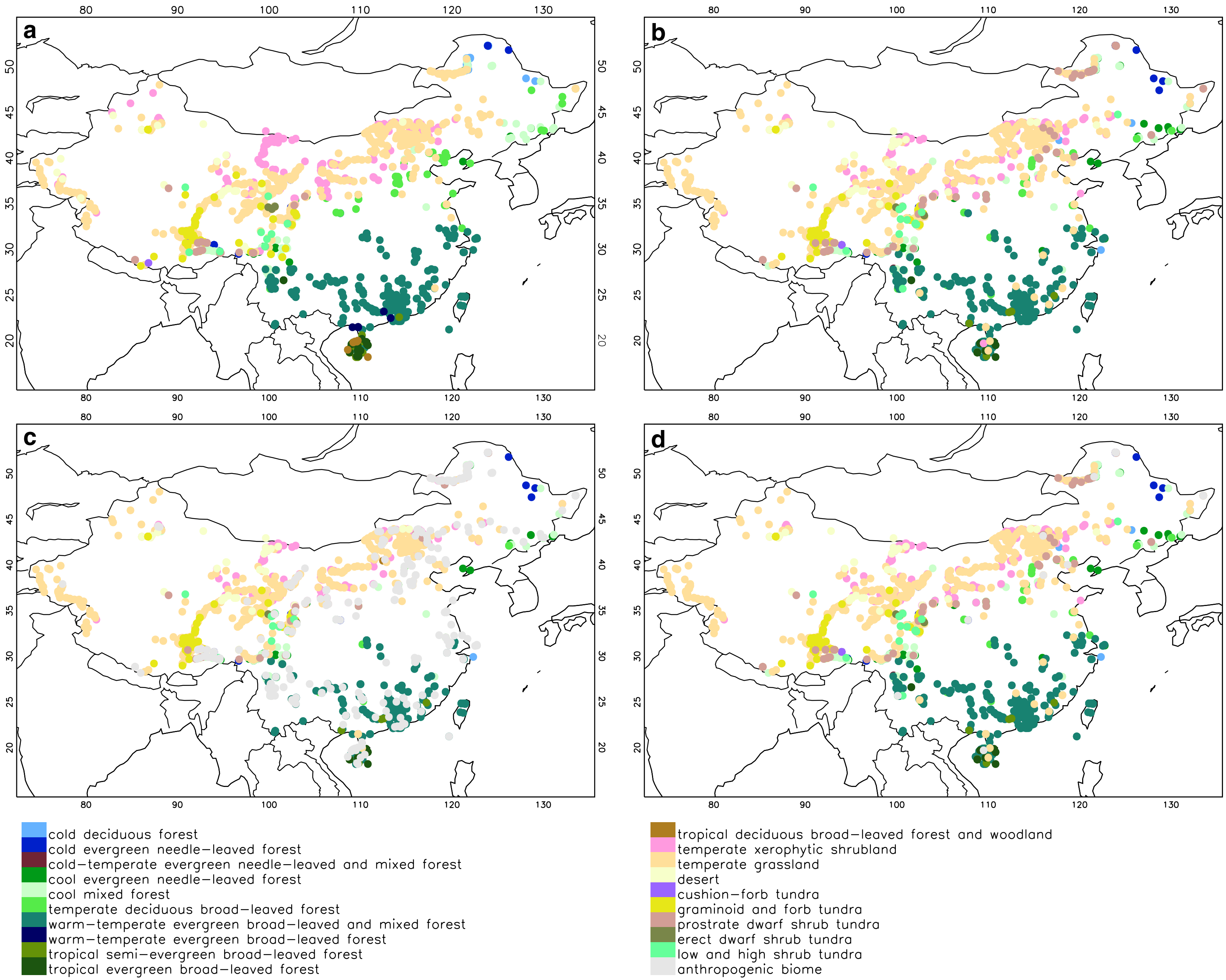

Fig. 2. Surface pollen-based modern biome distribution in China (a) derived from field observations and vegetation atlas (Editorial Board of Vegetation Atlas of China, Chinese Academy of Sciences, 2001) and (b) reconstructed using non-anthropogenic PFT assignment, (c) theoretical assignment of anthropogenic PFTs, and (d) assignment of anthropogenic PFTs in between the theoretical and practical setups. The restricted, practical assignment of anthropogenic PFTs produced the same biome pattern as the non-anthropogenic PFT assignment (b).

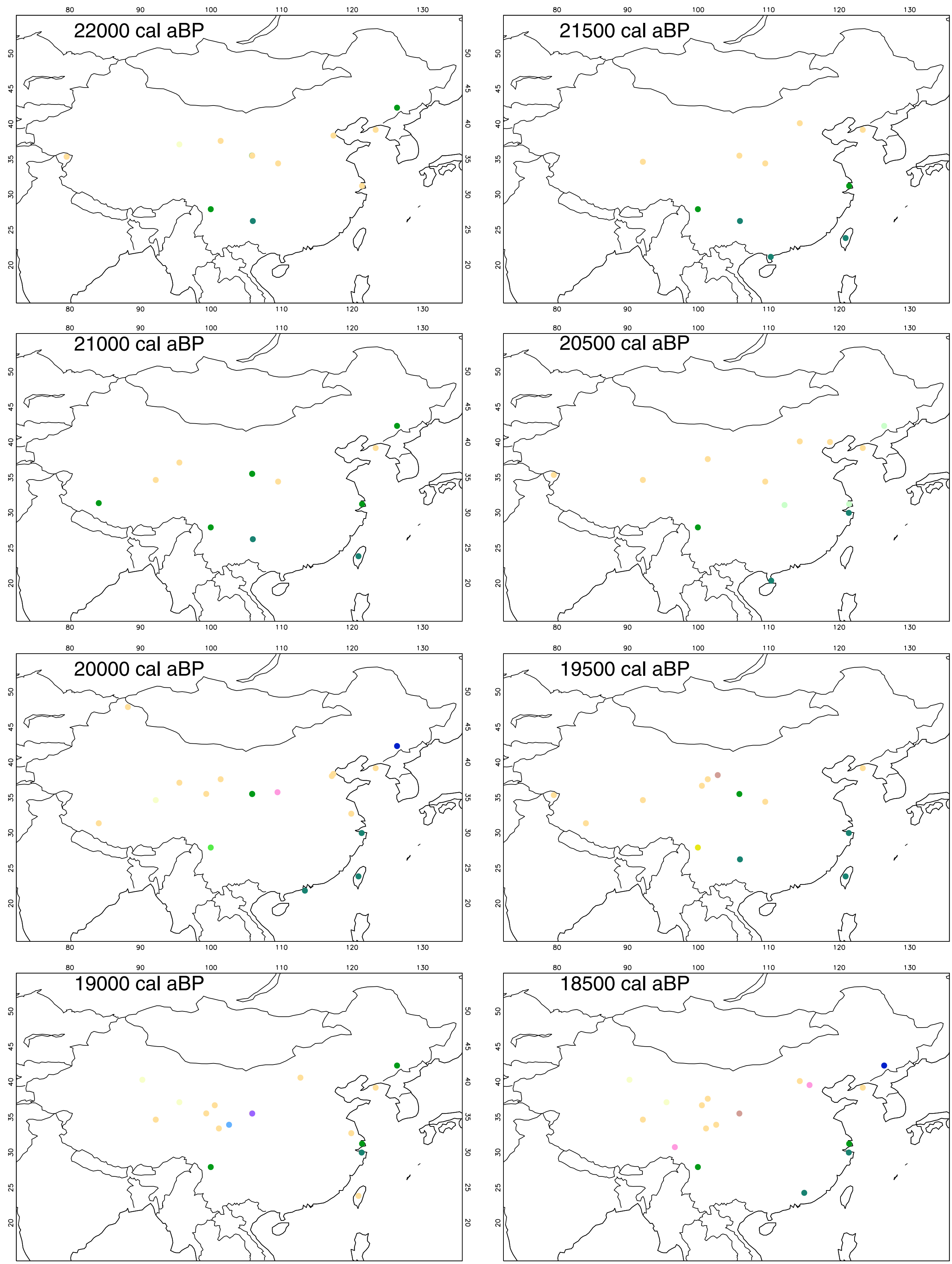

Fig. 3. Biome patterns in China during the last 22,000 yr.

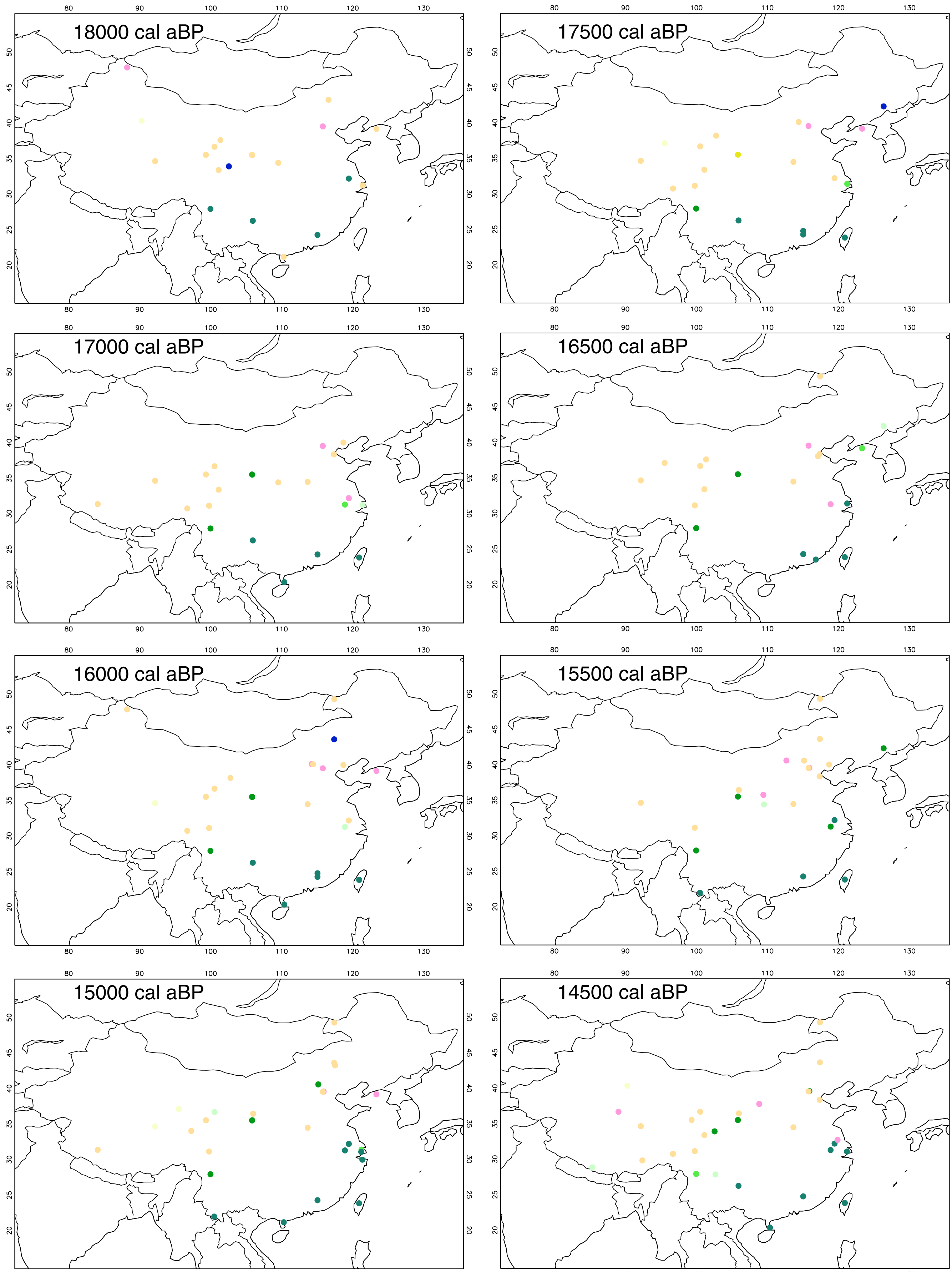

Fig. 3 (*continued*).

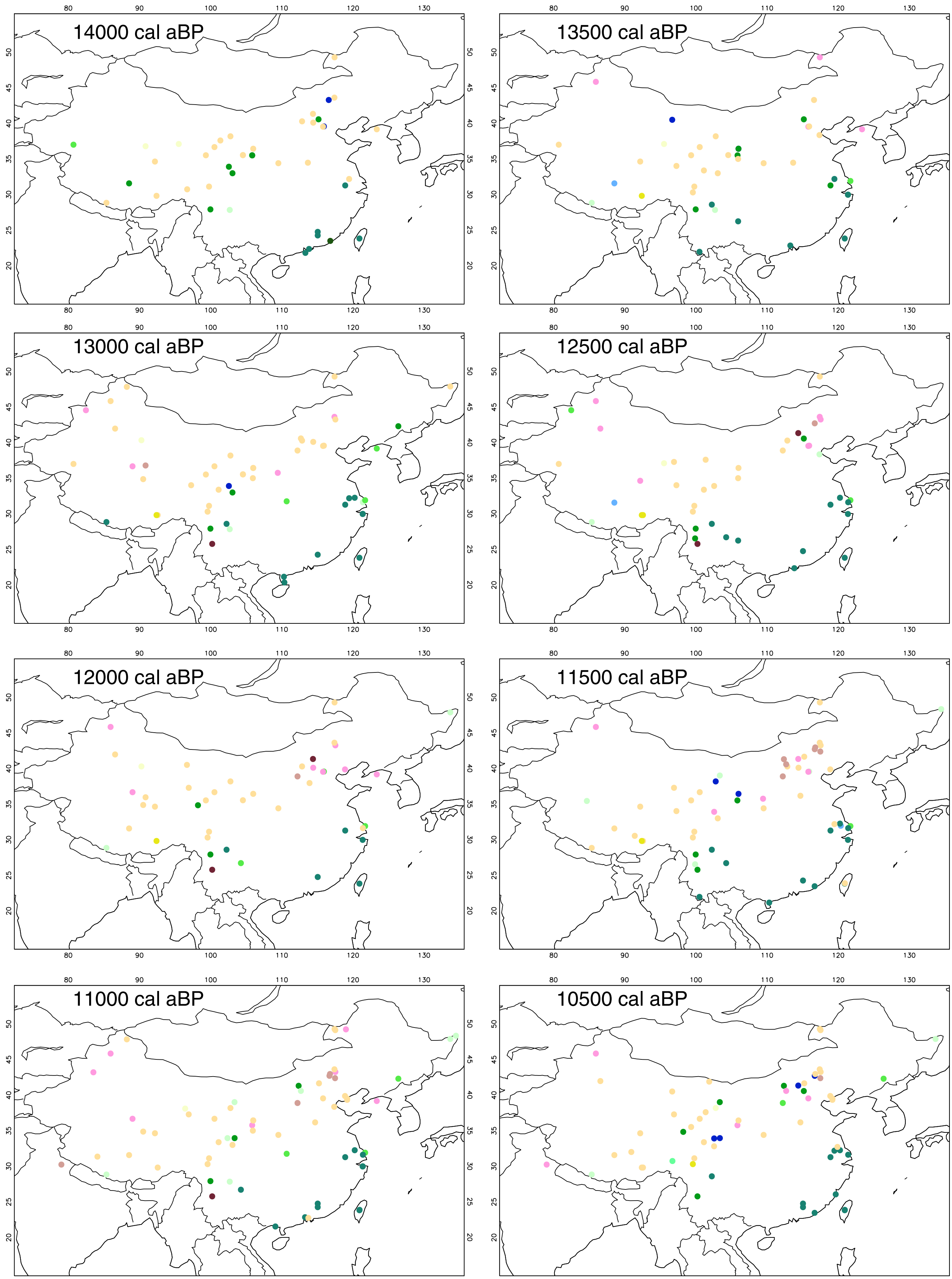

Fig. 3 (*continued*).

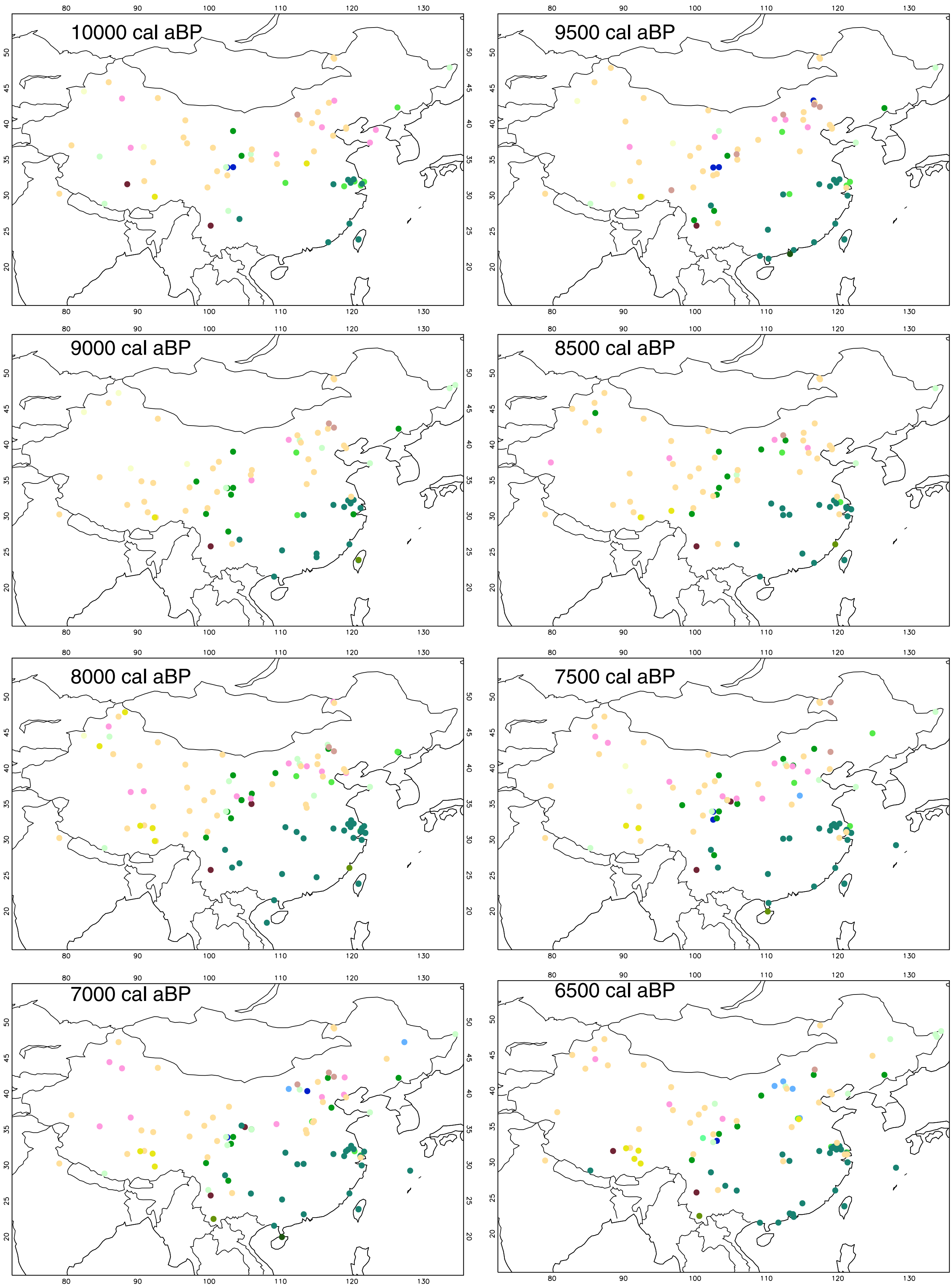

Fig. 3 (*continued*).

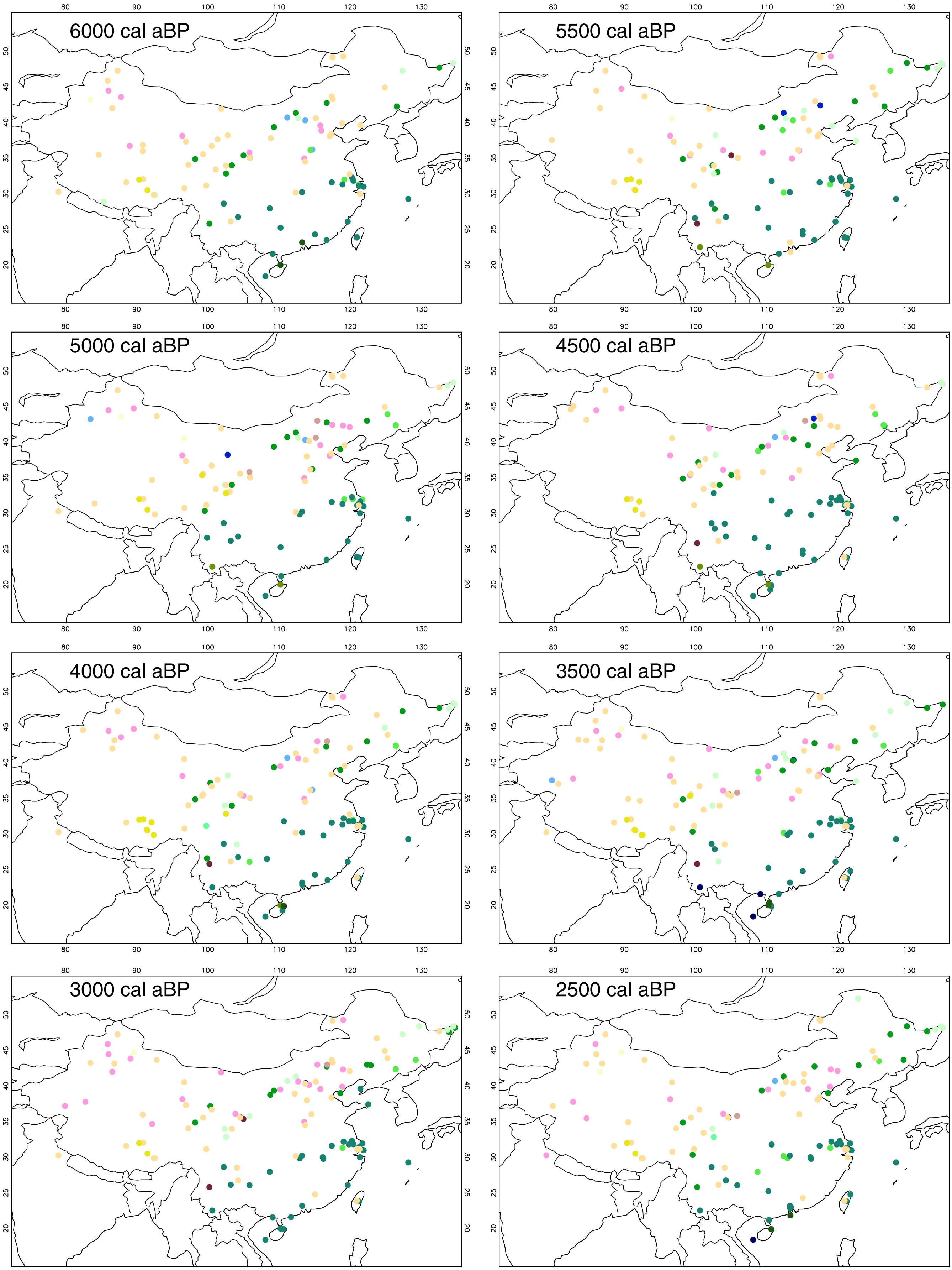

Fig. 3 (*continued*).

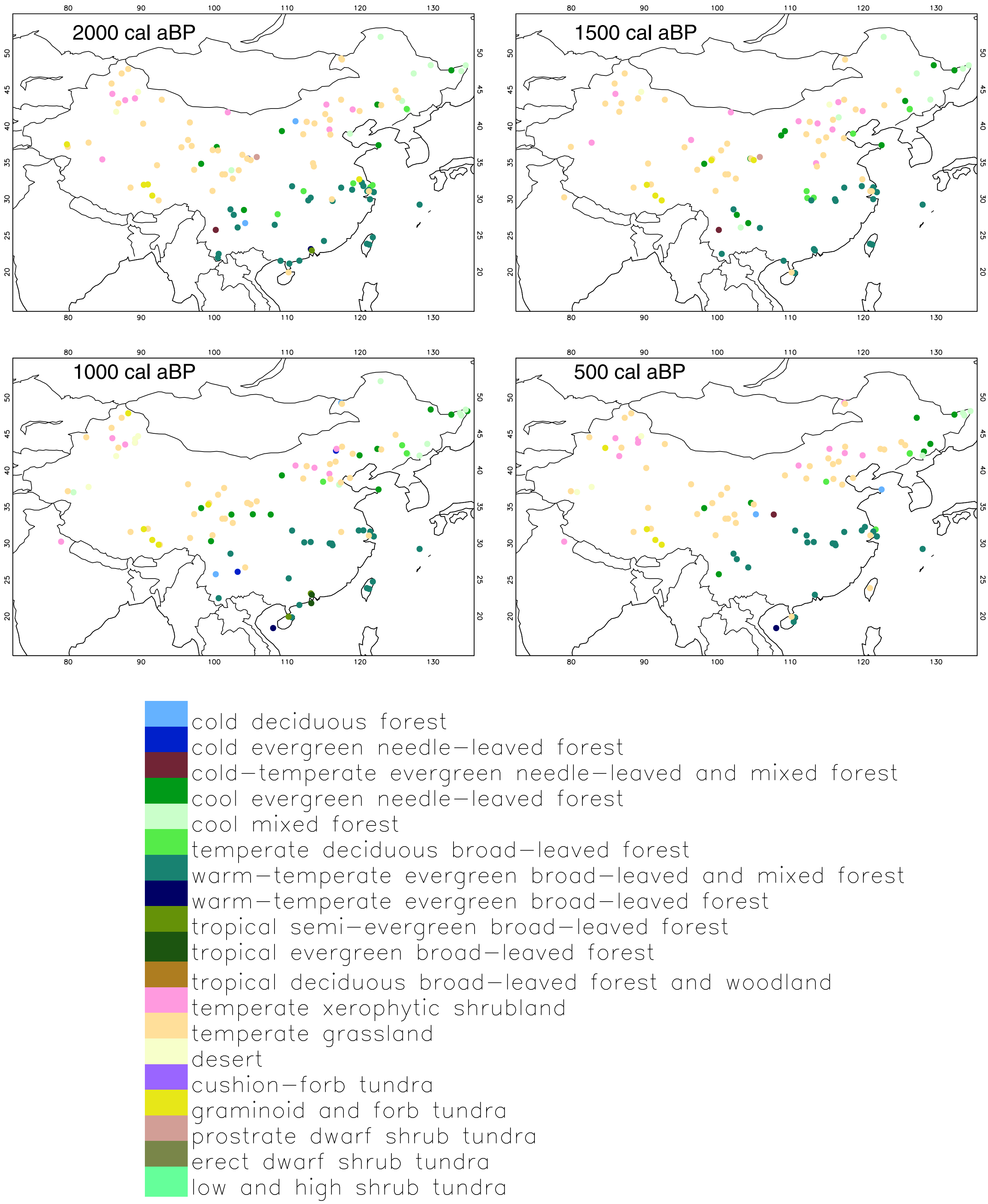

Fig. 3 (*continued*).

southern coastal areas. Forest biomes displayed a weak trend of a shift to the north, whereas temperate steppe and shrubland expanded to the north and west (Fig. 3 and Appendix 3).

3.2.4. MH (8.5 ka to 5.5 ka)

Forest biomes expanded to their largest ranges, but temperate steppe, xerophytic shrubland, and desert significantly reduced their ranges. Graminoid and forb tundra consistently occurred in the southeastern part of the Tibetan Plateau. More cold and cool forest biomes occupied the marginal areas of the Tibetan Plateau and high mountains in western China. Cold, cool, and temperate forests occupied a very large area at the ecotone between the forest and grassland biomes of central to northern and northeastern China, where temperate steppe and xerophytic shrubland previously occurred. Subtropical evergreen forest slightly shifted to the north and southwest, especially during the early MH. Tropical evergreen and semi-evergreen forests occupied southern and southwestern China, but shifted to the southern subtropical coast during the early MH. From 5.5 ka, the cold, cool, and temperate forest biomes commenced a weak shift southward and eastward (Fig. 3 and Appendix 3).

3.2.5. MH to Late Holocene (5 ka to 0.5 ka)

During the late period of MH, forest biomes further shifted back to the south and east. More cold or cool evergreen needle-leaved and temperate deciduous forests existed around the forest–grassland ecotone in central to northern China. Temperate grassland and xerophytic shrubland significantly expanded to the south and east, as well as in western China and on the Tibetan Plateau. Tropical forests often appeared in southern and southwestern China. From the late Holocene at 3 ka, no forest biomes were present in western China and on the surface of the Tibetan Plateau. Biome patterns during the late period of the late Holocene were similar to the distribution of modern biomes, but between 2.5 ka and 1.5 ka, temperate deciduous forest and a few cold or cool forests were largely distributed in the northern part of subtropical China, thus indicating a slight regional southward shift. Notably, several sites in subtropical southern China and a couple of sites in the eastern temperate zone were reconstructed to temperate grassland, likely indicating human disturbances, such as deforestation or local vegetation effects (Fig. 3 and Appendix 3).

Some key sites show dramatic biome shifts during the last 22 ka BP. For example, at the ecotone between forest and grassland in northern China (between 111–113°E and 38–42°N) four lakes reveal a shift between cold or cool forests and temperate steppe or xerophytic shrubland (Fig. 4a). In the transitional zone between the temperate and warm-temperate (subtropical), pollen records of three sites (119–122°E, 31–32°N) indicate a shift between temperate deciduous forest and warm-temperate evergreen mixed forest during the Holocene (Fig. 4b). Two sites in tropical southeastern and southwestern China show biome shifts between tropical semi-evergreen and evergreen forests, as well as between subtropical evergreen mixed and tropical semi-evergreen forests, during the middle to late Holocene (Fig. 4c). However, the eastern margin of the Tibetan Plateau shows more complicated biome changes throughout 22 ka BP (Fig. 4d). Two lakes in the southeastern margin (100–103°E, 28°N) indicate a shift between cool evergreen needle-leaved and cool mixed forests with the occasional presence of temperate deciduous and subtropical evergreen forests.

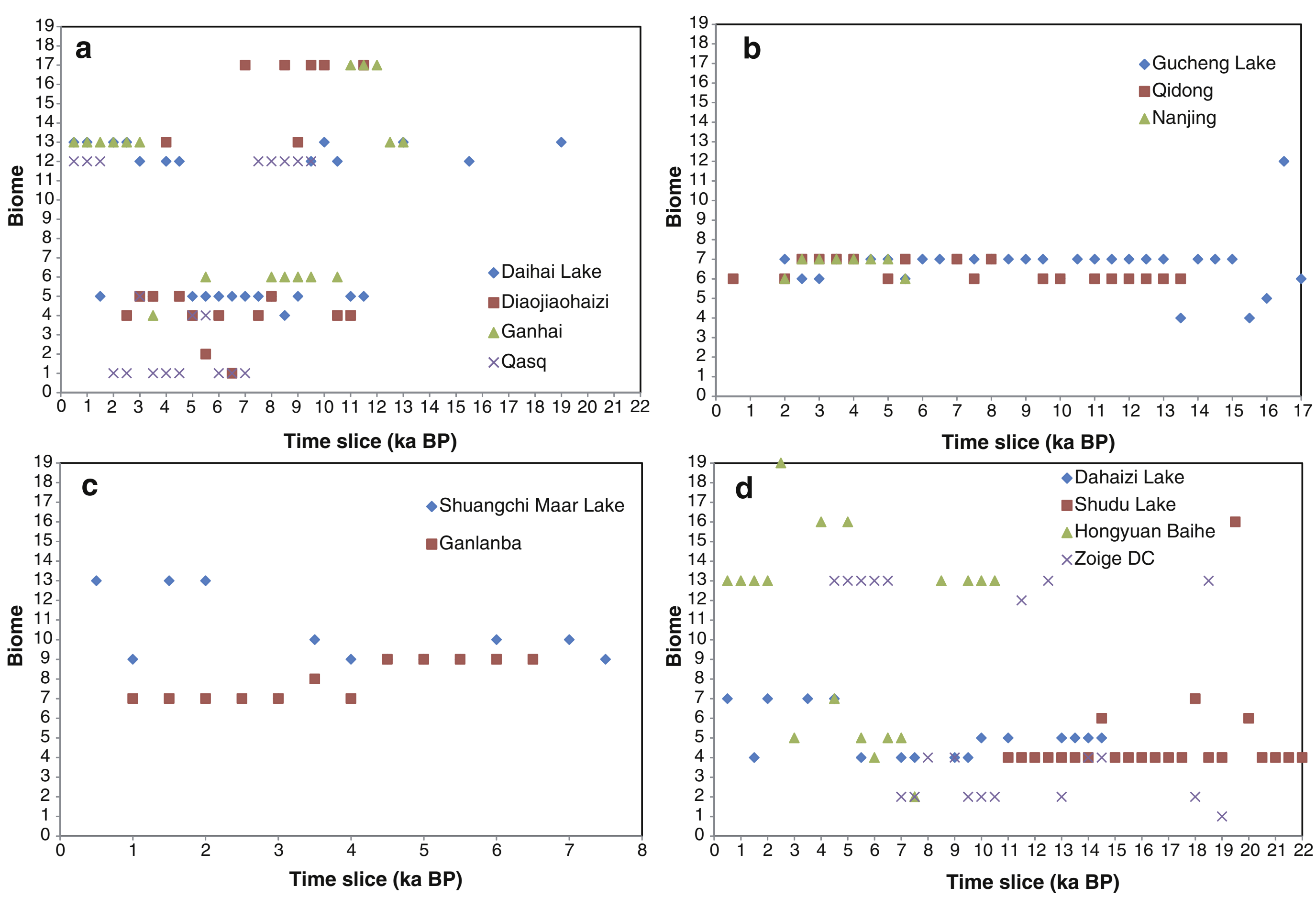

Fig. 4. Dramatic biome shifts in some sites at transitional zones. (a) Forest-grassland ecotone in northern China; (b) temperate–subtropical transitional zone in eastern China; (c) subtropical–tropical transitional zone in southeastern and southwestern China; and (d) Tibetan plateau margins. The number of biome can be found in Table 1.

Additionally, two peat sites in the middle eastern margin (103°E, 33–34°N) indicate a shift between cold or cool forests and temperate grassland or alpine tundra (Fig. 4d).

4. Discussion

4.1. Quality of pollen data used in this study

The number of surface pollen records is apparently sufficient for modern biome reconstruction, although large geographical gaps of sampling exist in central and western China (Fig. 1a), and further data collection is still required. More recent collection of modern pollen data at regional scales, such as on the Tibetan Plateau (Lu et al., 2011; Zhang et al., 2012), arid and semi-arid northern to western China (Zhao et al., 2012), the South China Sea (Luo et al., 2013), and throughout China (Zheng et al., 2010), are not or not wholly included in our dataset. However, fossil pollen data are necessary and required for more unambiguous reconstruction of biome boundaries, especially in central eastern China between temperate and warm–temperate (subtropical) forest biomes and in central western China between temperate desert and alpine tundra biomes (Fig. 1b). More fossil pollen records have been recently published but could not be obtained. Thus, raw data collection from palynologists of China and the western world will be a challenge in future paleovegetation research. On the one hand, both modern pollen data and fossil records must be collected to make the reconstructed biome boundaries accurate and unambiguous. On the other hand, the availability of relatively undisturbed and disturbed sites must be equally considered in future data sampling and collection, especially for modern pollen data.

The pollen dataset used in this study is of a higher quality than that used in previous studies. First, the dataset includes the entire sediments for the time-series biome reconstructions from 22,000 cal a BP to the present. Previous paleobiome reconstructions in China using the biomization technique focused only on the MH and LGM time slices (Yu et al., 1998, 2000; Ni et al., 2010). Second, our dataset has more accurate and calibrated radiocarbon dates. The mapping time slices are selected within a ± 150 yr time span. In previous works, the MH and LGM pollen samples were selected subjectively by choosing the samples with the nearest radiocarbon dating data to the MH and LGM. Radiocarbon dating data were not calibrated, but controlled based on the COHMAP dating control scheme (Webb, 1985). The MH was dated to 6000 ^{14}C a BP ± 500 yr and the LGM 18,000 ^{14}C a BP ± 2000 yr, which were both lower in temporal resolution than those in the present study. A disadvantage of our current pollen dataset is that more digitized pollen records have been used. Pollen records used in previous works were either digitized from publications (Yu et al., 1998) or combined digitized and raw data, but raw data accounted for ca. 80% of total records (Yu et al., 2000; Ni et al., 2010). In our study, some previously used sampling sites have been deleted from the current biomization procedure because of either the lack of radiocarbon dating or low resolution of pollen counts (Cao et al., 2013). The raw data records in our study account for ca. 50% of the total number of pollen sampling sites.

4.2. Paleobiome reconstruction

Many studies have indicated that past vegetation changes were synchronized with past climate changes, although vegetation displayed time lags in responding to climate changes. The previous reconstruction of paleobiome in China during the LGM and in the MH has shown that biome change was parallel in responding to multi-proxy record-based climate changes (Ni et al., 2010). Currently available past climate data are too limited to interpolate statistically the synchronized relationship between climate changes and specific biomes, but some plausible evidence has inferred the synchronized changes in both biome and climate. At the LGM, multi-proxy evidence shows a consistently weaker summer but stronger winter monsoon with colder and drier climates relative to today (Herzschuh, 2006; Shakun and Carlson, 2010; Bartlein et al., 2011; Clark et al., 2012). Cold and dry biomes (tundra, steppe, xerophytic shrubland, and desert) occupied a very large area of central to northern China. Forest biomes shifted remarkably southward, and no tropical forests were present in southern China during the entire LGM. Such biome distribution was consistent with global biome geography (Prentice et al., 2000). During deglaciation, climate transformed from the cold Oldest Dryas to warm Bølling–Allerød and cold Younger Dryas (Wang et al., 2010). Biomes weakly changed in some regions corresponding to climate transformation, but no large-scale shifts occurred at the regional scale. Eastward and southward expansion of temperate steppe and grassland and forest biomes that are located more southerly than their modern ranges were the common features during these three climate periods.

Climate during the Holocene in China is similar to the global trend, but subject to regional variations and timing differences (Shi et al., 1993; Feng et al., 2006; Herzschuh, 2006; Chen et al., 2008; Wang et al., 2010; Lu et al., 2011). During the cooler early Holocene, biomes in China were relatively similar to that in the Younger Dryas. In the later warmer and drier period, temperate steppe and xerophytic shrubland expanded to the north and west, and forest biomes slightly shifted to the north. The MH, which occurred in China at approximately 8 ka BP to 6 ka BP, was the warmest and wettest mega-thermal period (Shi et al., 1993). During this optimum climate period, forests in China flourished and expanded northward, representing their areas of largest distribution. However, temperate steppe, xerophytic shrubland, and desert shrank westward significantly. The strongest biome shifts occurred at 8 ka BP (Fig. 3). During the late Holocene, biome distributions weakly fluctuated in response to climate oscillations, from the early period of warmer and drier climates to the late period of cooler and wetter climates. Regional variations were observed in the timing and direction of biome fluctuations. Since approximately 6 ka BP to 5 ka BP, enhanced anthropogenic disturbances may have reduced forest cover in central to northern China (Ren, 2000). However, in our study, such forest degradation has not been reconstructed. Since 3 ka BP, the number of forest sites decreased (Fig. 3), possibly because of either intensive human disturbances or insufficient pollen records. More pollen data and historical documents are needed to answer fully the question of whether and how climate change or human disturbance-induced large-scale forest changes occurred during the late Holocene in China.

On the spatial scale of entire China, climate changes generally caused biome shifts in a similar manner, i.e., biomes shifted in the same direction under the same climate change event. However, the changes in biome range and area varied in different biomes, especially in terms of the positions of biome boundaries, indicating that the speed of shifts differed among biomes. Regional and local variation in biome shifts in both directions and ranges existed throughout the past 22,000-year period.

4.3. Anthropogenic biome reconstruction based on pollen records

The anthropogenic biome is a key to understanding the modern Earth system because 75% of Earth's land has been disturbed by humans (Alessa and Chapin, 2008; Ellis and Ramankutty, 2008; Ellis et al., 2010; Ellis, 2011). China has a long history of agricultural and forestry activities, such that the reconstruction of the anthropogenic biome is essential to understanding past vegetation, environment, and human interactions. However, the current assigned anthropogenic PFTs have little power in the construction of the anthropogenic biome.

Human activity has numerous pollen indicators (Li et al., 2008), particularly the pollen of anthropogenic weeds (e.g., Asteraceae, Brassicaceae, Caryophyllaceae, Fabaceae, Lamiaceae, Poaceae, and Scrophulariaceae) and food, fiber, oil, fruit, and vegetables (e.g., Apiaceae, Amaryllidaceae, Cannabidaceae, Convolvulaceae, Cucurbitaceae, Fabaceae, Poaceae, Solanaceae, and Rosaceae). Pollen indicators can be used for site-based and/or qualitative vegetation reconstructions. However, in broad-scale research, especially quantitative studies, these indicators were difficult to distinguish clearly from non-anthropogenic pollen at the same genus and family levels.

Some key pollen taxa, which should be strongly affected by human beings, cannot be assigned to one of three anthropogenic PFTs. Numerous crop and vegetable plants belong to the families of Chenopodiaceae, Compositae, Brassicaceae, Poaceae, and Solanaceae and should belong to the disturbed PFT. However, many herbaceous and shrubby plants in these families, especially in the former three, are dominant or major components of steppe and desert vegetation in northern and northwestern China and on the Tibetan Plateau. If these families are theoretically assigned to the disturbed PFTs, many sites in steppe and desert areas were assigned to the anthropogenic biome (Fig. 2c, fossil data not shown), which is inaccurate in most cases. Only the taxa in these families were assigned to the disturbed PFT (Appendix 2) in cases in which these taxa have been exactly identified as crops (e.g., Cerealia, *Oryza*, *Oryza sativa*, *Fagopyrum*, and *Zea*) or vegetables (e.g., *Brassica* and *Solanum*). However, in many cases, no exact species-level identification of these crops and vegetables exists, thus making their accurate assignment to the disturbed PFT difficult. Poaceae pollen grain size can be separated into small (<30 μm to 40 μm) and large pollen (>30 μm to 40 μm, which is recognized as crop taxa), but such cases are rare in our pollen dataset.

Many plantations can be found in both modern and fossil pollen spectra, such as the common genera *Pinus* (in different bioclimatic zones), *Cunninghamia*, *Cupressus*, *Castanea*, and *Juglans*. In archeological sites, numerous taxa of woody and shrubby plantations, which are very common in human settlements, can also be found in pollen spectra, such as *Pinus*, *Ulmus*, *Salix*, *Populus*, *Fraxinus*, *Tilia*, *Rosa*, and *Syringa*. However, these disturbed taxa of plantations are difficult to separate from those grown under natural conditions. In Japanese biome reconstruction, only four pollen taxa (*Artemisia*, Chenopodiaceae, Compositae, and Poaceae) were used to define an herb PFT, which was further used to define disturbed vegetation successfully along with the secondary and plantation PFTs (Gotanda et al., 2008). Such reconstruction in Japan was not problematic because it did not involve herbaceous plant-dominated biomes (i.e., steppe, desert, and tundra), but this condition is not true for China's reconstruction.

The second problem is on the number of anthropogenic biomes and PFTs used. Only one general type of anthropogenic biome and three anthropogenic PFTs are used in this study. Given China's long history of human transformation of ecosystems, few anthropogenic biome and PFTs obviously hinder the detection of human impacts on ecosystems. In a pseudobiomization work about anthropogenic land-cover change in the UK, Fyfe et al. (2010) used six PFTs (including the disturbed pasture/meadow and arable) to determine 10 land covers. However, such study has very limited numbers of both pollen sites and pollen taxa, thus enabling the determination of anthropogenic land cover. Considering more than 1000 pollen taxa and more than 2000 pollen sites in China, as well as the aforementioned difficulties in assigning pollen taxa to more appropriate anthropogenic PFTs, the classification of more anthropogenic biomes or land covers in China based on pollen records is a future challenge.

The third problem is on the availability of both disturbed and undisturbed pollen sites, apart from the further requirement of more pollen samples. Most pollen samples from soil and lake surfaces were selectively collected from sites with less human disturbance, such as natural reserves. This condition might be an additional reason for the limited anthropogenic biome reconstruction. Furthermore, the imbalance in the current availability of pollen samples in relatively undisturbed sites and disturbed sites where sampling gaps exist, such as in the Central to North China Plains and in the Sichuan Basin (Fig. 1a), might bias toward underestimating the reconstruction of anthropogenic biomes. However, such biases cannot be statistically quantified and evaluated primarily because the method of reconstructing anthropogenic biomes has not been consolidated (see discussion mentioned above) and insufficient detailed information is available on human disturbances in pollen sampling sites (Chen et al., 2010). The tests of anthropogenic biome reconstruction (Fig. 2c and d) show that almost all sites of disturbed vegetation are located in the eastern part of China with high population density, which implies that the tested reconstruction method partially captures human disturbance and that the bias of the geographic distribution of samples toward the reconstruction of anthropogenic biome is not significantly strong.

5. Conclusions

Anthropogenic biomes at a broad scale are not reasonably reconstructed in this study by the pollen-based quantitative method, but the natural biome distribution in China is well reconstructed, and its pattern has changed spatially and temporally over the past 22,000 calibrated years. Dramatic biome shifts are reconstructed in some time slices with abrupt climate changes, especially in transitional vegetation zones between forests and grassland, between temperate and subtropical forests, and in high mountains.

Based on the pollen dataset from eastern continental Asia, apart from the numerical biome reconstruction in this paper, the migration of key pollen taxa is mapped. Modern climate is reconstructed by using transfer functions, and past climate is reconstructed by using both the transfer functions and inverse vegetation modeling. However, pollen data collection, especially in geographical gaps where no or very few pollen records exist, is always a challenge. Undisturbed and disturbed sites in modern pollen sampling are equally important. By contrast, to distinguish anthropogenic biomes from natural vegetation change effectively, a more distinct assignment of pollen taxa to anthropogenic PFTs, as well as more effective numerical and/or mechanistic techniques in building large-scale human disturbances, is required. The numbers of anthropogenic PFTs and biomes (or land covers) must be increased.

Supplementary data to this article can be found online at http://dx.doi.org/10.1016/j.palaeo.2014.04.023.

Acknowledgments

This study was funded by the German Research Foundation (DFG), and the data collection was partly supported by the National Natural Science Foundation of China (NSFC). We thank the many Chinese and international palynologists who provided the raw pollen data for the past 15 years. We also thank the two anonymous reviewers for their helpful comments on an early version of this manuscript.

References

Alessa, L., Chapin III, F.S., 2008. Anthropogenic biomes: a key contribution to Earth-system science. Trends Ecol. Evol. 23, 529–531.
Bartlein, P.J., Harrison, S.P., Brewer, S., Connor, S., Davis, B.A.S., Gajewski, K., Guiot, J., Harrison-Prentice, T.I., Henderson, A., Peyron, O., Prentice, I.C., Scholze, M., Seppä, H., Shuman, B., Sugita, S., Thompson, R.S., Viau, A.E., Williams, J., Wu, H., 2011. Pollen-based continental climate reconstructions at 6 and 21 ka: a global synthesis. Clim. Dyn. 37, 775–802.
Cao, X.Y., Ni, J., Herzschuh, U., Wang, Y.B., Zhao, Y., 2013. A late Quaternary pollen dataset from eastern continental Asia for vegetation and climate reconstructions: set up and evaluation. Rev. Palaeobot. Palynol. 194, 21–37.
Chen, F.H., Yu, Z.C., Yang, M.L., Ito, E., Wang, S.M., Madsen, D.B., Huang, X.Z., Zhao, Y., Sato, T., Birks, H.J.B., Boomer, I., Chen, J.H., An, C.B., Wünnemann, B., 2008. Holocene moisture evolution in arid central Asia and its out-of-phase relationship with Asian monsoon history. Quat. Sci. Rev. 27, 351–364.
Chen, Y., Ni, J., Herzschuh, U., 2010. Quantifying modern biomes based on surface pollen data in China. Glob. Planet. Chang. 74, 114–131.
Clark, P.U., Shakun, J.D., Baker, P.A., Bartlein, P.J., Brewer, S., Brook, E., Carlson, A.E., Cheng, H., Kaufman, D.S., Liu, Z.Y., Marchitto, T.M., Mix, A.C., Morrill, C., Otto-Bliesner, B.L., Pahnke, K., Russell, J.M., Whitlock, C., Adkins, J.F., Blois, J.L., Clark, J., Colman, S.M., Curry, W.B., Flower, B.P., He, F., Johnson, T.C., Lynch-Stieglitz, J., Markgraf, V., McManus, J., Mitrovica, J.X., Moreno, P.I., Williams, J.W., 2012. Global climate evolution during the last deglaciation. Proc. Natl. Acad. Sci. U. S. A. 109, E1134–E1142.
Dearing, J.A., 2006. Climate–human–environment interactions: resolving our past. Clim. Past 2, 187–203.
Editorial Board of Vegetation Atlas of China, Chinese Academy of Sciences, 2001. Vegetation Atlas of China. Science Press, Beijing (In Chinese).

Ellis, E.C., 2011. Anthropogenic transformation of the terrestrial biosphere. Philos. Trans. R. Soc. A Math. Phys. Eng. Sci. 369, 1010–1035.

Ellis, E.C., Ramankutty, N., 2008. Putting people on the map: anthropogenic biomes of the world. Front. Ecol. Environ. 6, 439–447.

Ellis, E.C., Klein Goldewijk, K., Siebert, S., Lightman, D., Ramankutty, N., 2010. Anthropogenic transformation of the biomes, 1700 to 2000. Glob. Ecol. Biogeogr. 19, 589–606.

Feng, Z.D., An, C.B., Wang, H.B., 2006. Holocene climatic and environmental changes in the arid and semi-arid areas of China: a review. The Holocene 16, 119–130.

Fyfe, R., Roberts, N., Woodbridge, J., 2010. A pollen-based pseudobiomisation approach to anthropogenic land-cover change. The Holocene 20, 1165–1171.

Gaillard, M.-J., Sugita, S., Mazier, F., Trondman, A.-K., Brostrom, A., Hickler, T., Kaplan, J.O., Kjellstrom, E., Kokfelt, U., Kunes, P., Lemmen, C., Miller, P., Olofsson, J., Poska, A., Rundgren, M., Smith, B., Strandberg, G., Fyfe, R., Nielsen, A.B., Alenius, T., Balakauskas, L., Barnekow, L., Birks, H.J.B., Bjune, A., Bjorkman, L., Giesecke, T., Hjelle, K., Kalnina, L., Kangur, M., van der Knaap, W.O., Koff, T., Lageras, P., Latalowa, M., Leydet, M., Lechterbeck, J., Lindbladh, M., Odgaard, B., Peglar, S., Segerstrom, U., von Stedingk, H., Seppa, H., 2010. Holocene land-cover reconstructions for studies on land cover-climate feedbacks. Clim. Past 6, 483–499.

Gotanda, K., Nakagawa, T., Tarasov, P.E., Yasuda, Y., 2008. Disturbed vegetation reconstruction using the biomization method from Japanese pollen data: modern and Late Quaternary samples. Quat. Int. 184, 56–74.

Harrison, S.P., Prentice, I.C., Barboni, D., Kohfeld, K., Ni, J., Sutra, J.-P., 2010. Ecophysiological and bioclimatic foundations for a global plant functional classification. J. Veg. Sci. 21, 300–317.

Herzschuh, U., 2006. Palaeo-moisture evolution at the margins of the Asian monsoon during the last 50 ka. Quat. Sci. Rev. 25, 163–178.

Herzschuh, U., Tarasov, P., Wünnemann, B., Hartmann, K., 2004. Holocene vegetation and climate of the Alashan Plateau, NW China, reconstructed from pollen data. Palaeogeogr. Palaeoclimatol. Palaeoecol. 211, 1–17.

Herzschuh, U., Kurschner, H., Battarbee, R., Holmes, J., 2006. Desert plant pollen production and a 160-year record of vegetation and climate change on the Alashan Plateau, NW China. Veg. Hist. Archaeobot. 15, 181–190.

Kaplan, J.O., Krumhardt, K.M., Ellis, E.C., Ruddiman, W.F., Lemmen, C., Klein Goldewijk, K., 2011. Holocene carbon emissions as a result of anthropogenic land cover change. The Holocene 21, 775–791.

Kramer, A., Herzschuh, U., Mischke, S., Zhang, C., 2010. Holocene treeline shifts and monsoon variability in the Hengduan Mountains (southeastern Tibetan Plateau), implications from palynological investigations. Palaeogeogr. Palaeoclimatol. Palaeoecol. 286, 23–41.

Li, Y.Y., Zhou, L.P., Cui, H.T., 2008. Pollen indicators of human activity. Chin. Sci. Bull. 53, 1281–1293.

Lu, H.Y., Wu, N.Q., Liu, K.-B., Zhu, L.P., Yang, X.D., Yao, T.D., Wang, L., Li, Q., Liu, X.Q., Shen, C.M., Li, X.Q., Tong, G.B., Jiang, H., 2011. Modern pollen distributions in Qinghai–Tibetan Plateau and the development of transfer functions for reconstructing Holocene environmental changes. Quat. Sci. Rev. 30, 947–966.

Luo, C.X., Chen, M.H., Xiang, R., Liu, J.G., Zhang, L.L., Lu, J., Yang, M.X., 2013. Characteristics of modern pollen distribution in surface sediment samples for the northern South China Sea from three transects. Quat. Int. 286, 148–158.

Ni, J., Yu, G., Harrison, S.P., Prentice, I.C., 2010. Palaeovegetation in China during the late Quaternary: biome reconstructions based on a global scheme of plant functional types. Palaeogeogr. Palaeoclimatol. Palaeoecol. 289, 44–61.

Prentice, I.C., Webb III, T., 1998. BIOME 6000: reconstructing global mid-Holocene vegetation patterns from palaeoecological records. J. Biogeogr. 25, 997–1005.

Prentice, I.C., Guiot, J., Huntley, B., Jolly, D., Cheddadi, R., 1996. Reconstructing biomes from palaeoecological data: a general method and its application to European pollen data at 0 and 6 ka. Clim. Dyn. 12, 185–194.

Prentice, I.C., Jolly, D., BIOME 6000 participants, 2000. Mid-Holocene and glacial-maximum vegetation geography of the northern continents and Africa. J. Biogeogr. 27, 507–519.

Ren, G.Y., 2000. Decline of the mid-to late Holocene forests in China: climatic change or human impact? J. Quat. Sci. 15, 273–281.

Shakun, J.D., Carlson, A.E., 2010. A global perspective on Last Glacial Maximum to Holocene climate change. Quat. Sci. Rev. 29, 1801–1816.

Shi, Y.F., Kong, Z.C., Wang, S.M., Tang, L.Y., Wang, F.B., Yao, T.D., Zhao, X.T., Zhang, P.Y., Shi, S.H., 1993. Mid-Holocene climates and environments in China. Glob. Planet. Chang. 7, 219–233.

Wang, Y.B., Liu, X.Q., Herzschuh, U., 2010. Asynchronous evolution of the Indian and East Asian Summer Monsoon indicated by Holocene moisture patterns in monsoonal central Asia. Earth Sci. Rev. 103, 135–153.

Webb III, T., 1985. A global paleoclimatic data base for 6000 yr B.P. TRO 18, DOE/EV/10097-6. U.S. Department of Energy, Washingtong, DC.

Woodbridge, J., Fyfe, R.M., Roberts, N., Downey, S., Edinborough, K., Shennan, S., 2014. The impact of the Neolithic agricultural transition in Britain: a comparison of pollen-based land-cover and archaeological ^{14}C date-inferred population change. J. Archaeol. Sci. http://dx.doi.org/10.1016/j.jas.2012.10.025.

Yu, G., Prentice, I.C., Harrison, S.P., Sun, X., 1998. Pollen-based biome reconstruction for China at 0 and 6000 years. J. Biogeogr. 25, 1055–1069.

Yu, G., Chen, X., Ni, J., Cheddadi, R., Guiot, J., Han, H., Harrison, S.P., Huang, C., Ke, M., Kong, Z., Li, S., Li, W., Liew, P., Liu, G., Liu, J., Liu, K.-B., Prentice, I.C., Qui, W., Ren, G., Song, C., Sugita, S., Sun, X., Tang, L., van Campo, E., Xia, Y., Xu, Q., Yan, S., Yang, X., Zhao, J., Zheng, Z., 2000. Palaeovegetation of China: a pollen data-based synthesis for the mid-Holocene and last glacial maximum. J. Biogeogr. 27, 635–664.

Zhang, S., Xu, Q., Nielsen, A.B., Chen, H., Li, Y., Li, M., Hun, L., Li, J., 2012. Pollen assemblages and their environmental implications in the Qaidam Basin, NW China. Boreas 41, 602–613.

Zhao, Y., Liu, H.Y., Li, F.R., Huang, X.Z., Sun, J.H., Zhao, W.W., Herzschuh, U., Tang, Y., 2012. Application and limitations of the Artemisia/Chenopodiaceae pollen ratio in arid and semi-arid China. The Holocene 22, 1385–1392.

Zheng, Y.W., Zheng, Z., Tarasov, P., Qian, L.X., Huang, K.Y., Wei, J.H., Luo, C.X., Xu, Q.H., Lu, H.Y., Luo, Y.L., 2010. Palynological and satellite-based MODIS observations of modern vegetational gradients in China. Quat. Int. 218, 190–201.